Original scientific paper

Relationship modelling for surface finish for laser-based additive manufacturing

Samidha Jawade✉and Ganesh Kakandikar

School of Mechanical Engineering School of Mechanical Engineering, Dr. Vishwanath Karad MIT World Peace University, Pune, Maharashtra, India

Corresponding author: ✉samidha.jawade@mitwpu.edu.in

Abstract

Nickel-based superalloys belong to a special class of high-performance alloys that feature large amounts of nickel. The uniqueness of superalloys lies in their design features, most notably mechanical strength, durability, etc. Inconel 718 (IN718) is a nickel-based superalloy that exhibits high tensile and impact-resistant properties, along with good high-temperature corrosion resistance. Selective Laser Melting (SLM) is additive manufacturing (AM) technology aimed at melting and fusing metal powders using high power density lasers to produce precision functional parts. The accuracy and functional characteristics of manufactured parts are highly dependent on process parameters. The processing parameters that control the SLM process comprise laser power (P), hatch spacing (HS), exposure time (t), and border power (BP). This work primarily focuses on finding the combined effect of these process parameters on the surface roughness (SR) and ultimate tensile strength (UTS) of IN718 manufactured by SLM using the design of experiments (DOE).

Keywords
Selective laser melting; mechanical properties; surface roughness; Inconel; superalloys

Introduction

Inconel 718 (IN718) is an age-hardenable nickel-based superalloy [1]. The aerospace, energy, and automotive industries are accelerating specific applications of AM technology in the manufacture of parts made of nickel-based superalloys [2,3]. The aerospace industry poses complicated techno-logical needs, metal to work in extreme conditions, including cryogenic and high temperatures. Because of these demands, Nickel-based superalloys have been developed. Applications for these materials are found in different areas like engine turbine blades, nuclear reactors, turbochargers, heat exchangers and petrochemical equipment *etc.* [4,5]. The IN718 alloys show outstanding malleability and weldability, high tensile, fatigue, creep, and rupture strength has led to its widespread application [6,7]. Previously, manufacturing industries depended upon subtractive manufacturing processes to make the products. Nowadays additive manufacturing processes are replacing them [8-10]. Additive manufacturing is the computer-controlled process of constructing a

3D object by joining layers of material with the help of a laser on a build platform till the final product is finished [11,12]. Today, in additive manufacturing, selective laser melting (SLM) is one of the promising technology available for rapid prototyping and mass production. The use of metal alloys in the SLM process to manufacture the parts used in different applications is limited [13-15].

For some reason, the industry is still hesitant to adopt the SLM process used for the mass production of critical components. The most important concerns are a surface finish, microstructural inhomogeneity and microstructural defects observed in SLM-generated parts that can affect mechanical properties badly [16,17].

The process parameters of selective laser melting play a huge role in determining the surface finish and the mechanical properties of the SLM manufactured component [18]. Although SLM offers great flexibility in design, the CAD geometry may get affected due to the changes in the process parameters [19,20]. Process parameters also play an important role in determining the type of the grain's size and shape, melt pools and composition of different phases, which in turn dictates the mechanical properties such as surface roughness, and tensile strengths of the fabricated parts [21,22]. Therefore, analysis of the process helps us understand the impact of these process parameters on microstructural and mechanical properties. This understanding of the process parameters shall provide feasibility to dynamically control the build process and thus, can be made more efficient, thereby reducing the microstructural defects [23]. This work mainly focused on the effect of process parameters to optimize the surface finish and mechanical properties of parts fabricated by SLM. Microstructural analyses are performed on the fabricated parts and they are followed by a mechanical investigation like surface roughness and strength. Finally, the study is concluded by co-relating the effect of Laser power, hatch spacing, exposure time, border power with the surface roughness (R_a) and mechanical properties of IN718.

Materials and methods

Materials and process parameters

Commercially available Renishaw In718-0405 in powder form is selected for experimentation. Based on the extensive literature review, the laser power, exposure time, border power and hatch distance were finally taken into consideration. Melting of powder is crucial in SLM and appropriate laser power ensures proper melting. Exposure time ensures homogeneous melting at each layer. There is the possibility of uneven melting at borders. Border power is an important parameter to ensure the same quality of melting at the surface as that of the core. Hatch distance/ spacing is the separation between two consecutive laser beams. Appropriate hatch distance ensures good quality of melting. As all the process parameters can be varied at three levels, and with the help of Taguchi's design of experiment, the resulting orthogonal array L9 was selected for the further process. Table 1 presents the selected parameters and their levels. Table 2 presents the L9 orthogonal array. Figure 1 shows the standard tensile test specimen drawing used for specimen manufacturing through the SLM process. The specimen was manufactured using Renshaw AM 400 machines, shown in Figure 2. Figure 3 shows the component manufactured as per the L9 array for the experimentation.

The optimization of process parameters in SLM processes is important as the process parameters affect the microstructural property, compositional property, mechanical property, geometrical accuracy, and surface finish of the fabricated parts. Over the years, very few researchers have tried to optimize these process parameters to reduce the variation and establish standard process parameters. As the SLM process is affected by many parameters, a trial-and-error method would require a large number of tests, which is not suitable as it would be difficult to determine the

correlation between a specific parameter and its desired value [18]. It must also be noted that this technique is time-consuming and expensive. Design of Experiments (DOE) techniques help as a practical alternative for the trial-and-error methods [19].
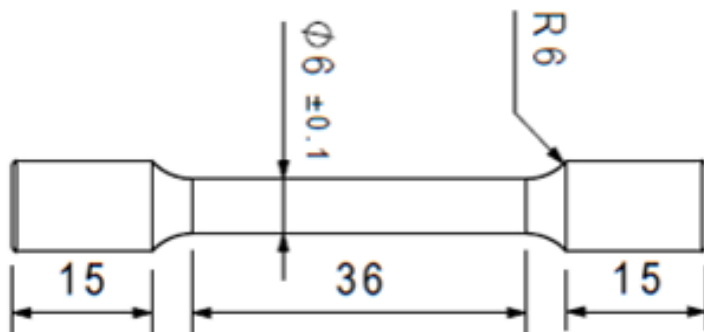

Figure 1. *Tensile sample (ASTM E8) manufactured by SLM*

Figure 2. *Renishaw AM 400 machine*

Figure 3. *Tensile test specimens in L9 experimentation*

Table 1. *SLM process parameters levels for manufacturing of tensile specimen*

Parameters	Level 1	Level 2	Level 3
Laser power, W	315	345	375
Hatching distance, μm	75	90	105
Exposer time, μs	15	20	25
Border power, W	275	325	375

Table 2. *L9 Array of different SLM process parameters*

Sr. No.	Power, W	Hatch spacing, μm	Exposer time, μs	Border power, W
1	315	75	15	275
2	315	90	20	325
3	315	105	25	375
4	345	75	20	375
5	345	90	25	275
6	345	105	15	325
7	375	75	25	325
8	375	90	15	375
9	375	105	20	275

Results and discussion

Performance measures

Surface roughness and tensile test were performed on selective laser melted Inconel 718 (IN718) specimens. The surface roughness is critical to its function and long-term performance. It is a key factor in mechanical properties and is driven by additive modality and process parameters. The surface finish influences the mechanical properties and aesthetics of components; hence surface roughness is part of the investigation. 2nd performance parameter was ultimate tensile strength. It is the maximum stress a material can withstand before breaking. Table 3, Figure 4 and Figure 5 indicate the results of nine experiments as well as process variability for both performance measures. It is observed that surface roughness (R_a values) varies between 8.46 μm to 9.51 μm. Surface roughness master was used to measure the surface roughness. Minimum surface roughness is observed in Experiment no 6 specimens. Ultimate tensile strength varies between 1045 to 1089 MPa. It is measured using universal testing machines. Minimum UTS was observed in the Exp 7 specimen and maximum UTS in experiment 9. Error bar of surface roughness and ultimate tensile strength are shown in Figures 6 and 7, respectively. Figure 8 shows the specimen after the tensile test.

Table 3. *Design of experiment – performance measures*

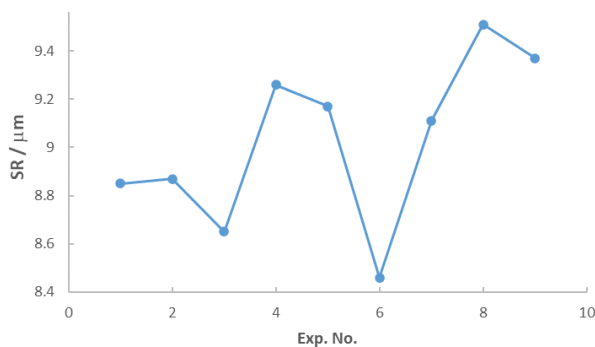| Sr. No.	P / W	HS / μm	t / μs	BP / W	SR / μm	UTS / MPa
1	315	75	15	275	8.85	1080
2	315	90	20	325	8.87	1078
3	315	105	25	375	8.65	1080
4	345	75	20	375	9.26	1081
5	345	90	25	275	9.17	1065
6	345	105	15	325	8.46	1059
7	375	75	25	325	9.11	1045
8	375	90	15	375	9.51	1082
9	375	105	20	275	9.37	1089

Figure 4. *Surface roughness of IN718 versus experiment number*
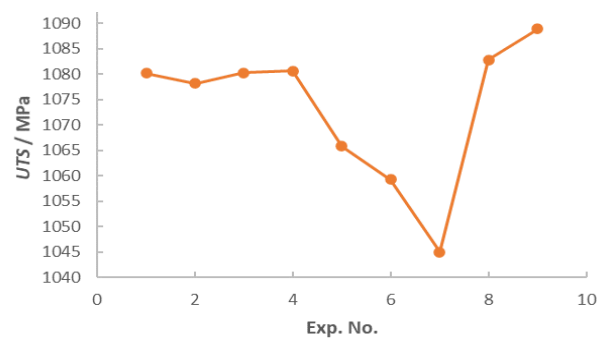
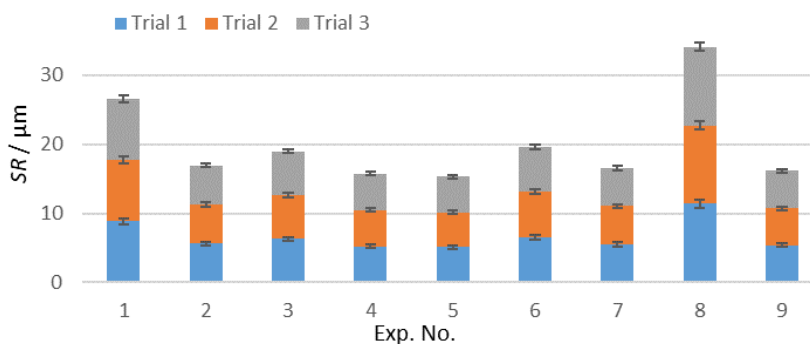***Figure 5.*** *Ultimate tensile strength of IN718 versus experiment number*

Figure 6. *Error bar of surface roughness IN718*

S. Jawade and G. Kakandikar

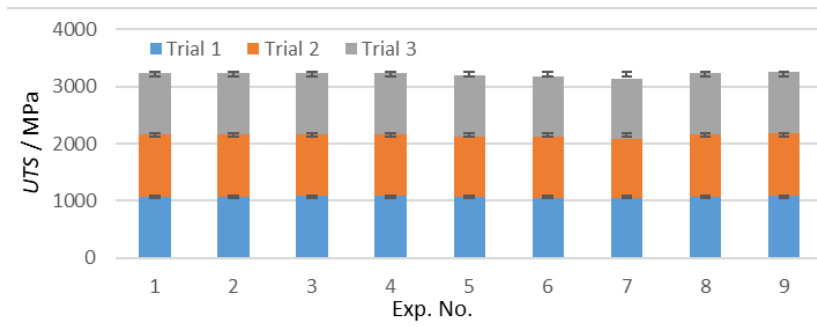*J. Electrochem. Sci. Eng.* **13(1)** (2023) 127-135

Figure 7. Error bar of ultimate tensile strength IN718

Figure 8. Specimens after tensile test

DOE Analysis

Results of the *S/N* ratio analysis, which indicate the influence of the process parameters i.e., laser power, exposure time, border power, and hatch spacing on the surface roughness and UTS of the SLM printed part, are presented in Table 4. The process parameters with strong influence were identified using the difference between the maximum and minimum value, *i.e.,* delta at the three levels in the experimentation.

Table 4. S/N ratio obtained after Taguchi analysis

Sr. No.	P / W	HS / µm	t / µs	BP / W	S/N ratio of SR	S/N ratio of UTS
1	315	75	15	275	-18.938	60.670
2	315	90	20	325	-18.958	60.654
3	315	105	25	375	-18.740	60.670
4	345	75	20	375	-19.332	60.673
5	345	90	25	275	-19.247	60.553
6	345	105	15	325	-18.547	60.499
7	375	75	25	325	-19.190	60.382
8	375	90	15	375	-19.563	60.691
9	375	105	20	275	-19.434	60.739

Tables 5 and 6 represent the crucial factors for surface roughness and UTS. For surface roughness, laser power is the most influential parameter as compared to the other three. It is observed that for UTS, border power is most influential, whereas exposure time has the second rank. The other two parameters are the least important. It was observed that laser power plays a big role in SLM manufactured IN718 parts to improve the surface roughness. The roughness analysis of SLM fabricated parts established that the high values for R_a were due to the presence of unmelted particles formed on the surface due to irregular melting and cooling processes. It was observed that maintaining the hatch spacing leads to a steady melt pool architecture, resulting in lower values for R_a. Balling effect also increases the surface roughness values and it can be reduced by the melting

and re-melting process which in turn enhances the values of R_a by around 80 %. The balling effect is a problem that frequently occurs in the selective laser melting forming process and seriously affects the surface precision of the manufactured part. Balling is a defect that can occur when the molten pool created during selective laser melting becomes discontinuous and breaks into separated islands.

Table 5. *Signal to noise for surface roughness*

Level	P / W	HS / μm	t / μs	BP / W
1	-18.88	-19.15	-19.02	-19.21
2	-19.04	-19.26	-19.24	-18.90
3	-19.40	-18.91	-19.06	-19.21
Delta	0.52	0.35	0.23	0.31
Rank	1	2	4	3

Table 6. *Response table of signal to noise for UTS*

Level	P / W	HS / μm	t / μs	BP / W
1	60.66	60.58	60.62	60.65
2	60.58	60.63	60.69	60.51
3	60.60	60.64	60.54	60.68
Delta	0.09	0.06	0.15	0.17
Rank	3	4	2	1

Microstructural analysis

The XRD spectrum of the IN 718 powder used as an interfacing layer is shown in Figure 9; the spectrum is coincident with a solid solution of austenite (g) face-centered cubic (fcc) Ni–Cr matrix and shows the dominant presence of (111) plane. For the XRD analysis, ULTIMA IV fully automated optical alignment machine was used. To examine the fracture surface FESEM – FEI Nova NanoSEM 450 machine was used. Fracture surfaces of the tensile specimen are shown in Figures 10 and 11. Experiment 9, tensile specimen showed ductile fracture characteristics, dimples on the fracture. In experiment 7, very small particle size was observed because of the non-equilibrium melting and solidification. Figure 11 shows the fractography after the tensile test of Experiment no 7-specimen investigation of the fractured samples revealed process-induced defects such as pores, unmelted and partially melted powder particles.
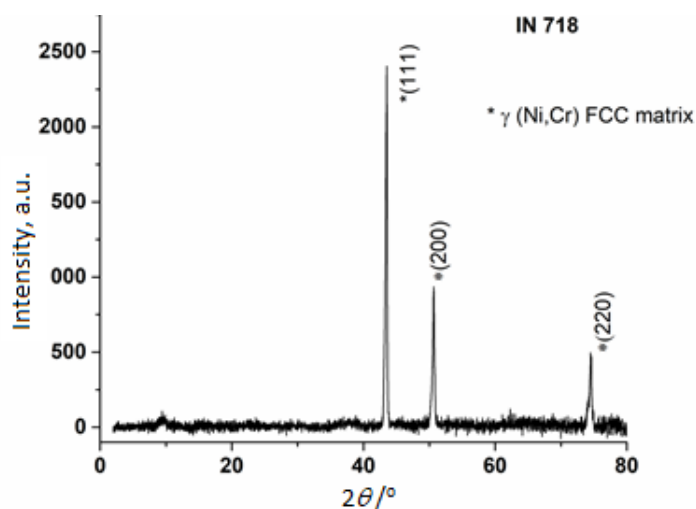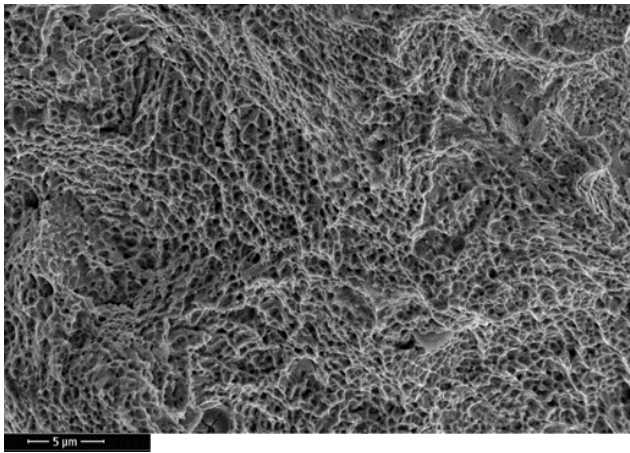

Figure 9. *XRD analysis of IN718*

S. Jawade and G. Kakandikar

J. Electrochem. Sci. Eng. **13(1)** (2023) 127-135

Figure 10. *Fractography of tensile specimen (IN718) of experiment No.9*
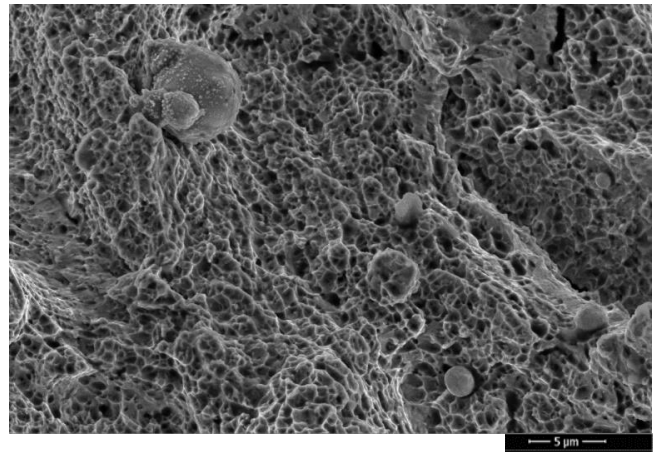

Figure 11. *Fractography of tensile specimen (IN718) of experiment No.7*

Figure 11 shows the fractography after the tensile test of Experiment no 7-specimen investigation of the fractured samples revealed process-induced defects such as pores, unmelted and partially melted powder particles. It is likely that these defects serve as stress raisers and eventually lead to crack initiation and failure. The micro-pore act as a crack initiator. In tensile tests, due to stress concentration, microcracks usually start at these weakest locations and then propagate to accelerate fracture.

Simulation

'Simufact' Additive 2021 is a powerful software solution for the simulation of selective laser melting. 3D CAD model of tensile specimen used for the simulation purpose, shown in Figures 12, 13 and 14. After that, the model is imported into simufact additive (SA) software to generate mesh, support and define the material properties. Simulation by changing process parameters was observed and experimental results were validated with the help of the simulation model. Experimental results and simulation result shows a good agreement.
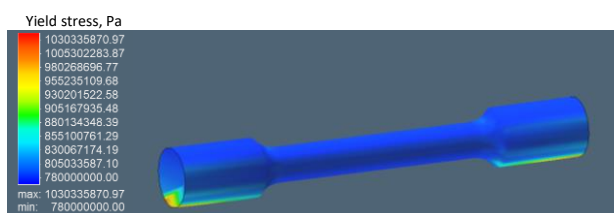

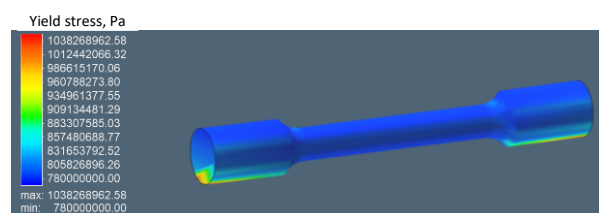***Figure 12.*** *The contour map showing the yield stress simulation result at 315 W*

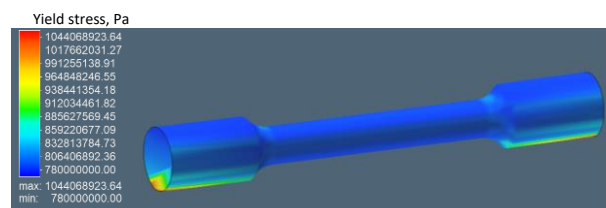***Figure 13.*** *The contour map showing the yield stress simulation result at 345 W*

Figure 14. *The contour map showing the yield stress simulation result at 375 W*

Conclusion

The objective of this research is to correlate the effect of process parameters on the properties of IN718 specimens using the Taguchi method. Surface roughness and ultimate tensile strength

(UTS) are considered as it facilitates the correlation between the process parameters and performance measures. The parameters most infusing the surface roughness of SLM manufactured IN718 parts are laser power and hatch spacing and for the UTS, border power and exposure time play a vital role. In microstructural analysis, it was observed that defects such as the presence of unmelted powder and balling effect had an impact on the mechanical properties such as UTS and surface roughness which are the focus of this research. Simulation and experimentally calculated values show a better agreement of both the performance measures. The slight variation may be due to randomness in the process.

References

[1]   W. M. Tucho, V. Hansen, *Journal of Materials Science* **54** (2019) 823-839. https://doi.org/10.1007/s10853-018-2851-x

[2]   Q. Jia, D. Gu, *Journal of Alloys and Compounds* **585** (2014)713-721. https://doi.org/10.1016/j.jallcom.2013.09.171

[3]   X. Liu, K. Wang, P. Hu, X. He, B. Yan, X. Zhao, *Materials* **14** (2021) 991. https://doi.org/10.3390/ma14040991

[4]   V. R. Rajendran, K. Mamidi, B. Ravichander, B. Farhang, A. Amerinatanzi, N. S. Moghaddam, Determination of residual stress for Inconel 718 samples fabricated through different scanning strategies in selective laser melting, *Behavior and Mechanics of Multifunctional Materials IX,* SPIE Smart Structures + Nondestructive Evaluation, Online, Proceedings Volume 11377, 2020, 1137719. https://doi.org/10.1117/12.2558342

[5]   Y. Lu, S. Wu , Y. Gan, T. Huang , C. Yang , L. Junjie , J. Lin, *Optics and Laser Technology* **75** (2015) 197–206. https://doi.org/10.1016/j.optlastec.2015.07.009

[6]   A. Jahadakbar, M. Nematollahi, K. Safaei, P. Bayati, G. Giri, H. Dabbaghi, D. Dean, M. Elahinia, *Metals* **10(1)** (2020) 151. https://doi.org/10.3390/met10010151

[7]   N. S. Moghaddam, S. E. Saghaian, A. Amerinatanzi, H. Ibrahim, P. Li, G. P. Toker, H. E. Karaca, M. Elahinia, *Materials Science and Engineering A* **724** (2018) 220-230. https://doi.org/10.1016/j.msea.2018.03.072

[8]   B. Farhang, B. B. Ravichander, F. Venturi, A. Amerinatanzi, N. S. Moghaddam, *Materials Science and Engineering A* **774** (2020) 138919. https://doi.org/10.1016/j.msea.2020.138919

[9]   N. S. Moghaddam, A. Jahadakbar, A. Amerinatanzi, M. Elahinia, *Recent Advances in Laser-Based Additive Manufacturing* in *Laser-Based Additive Manufacturing of Metal Parts,* L. Bian, N. Shamsaei, J. M. Usher, Eds., CRC Press, Boca Raton, USA, 2017),1-24. https://doi.org/10.1201/9781315151441

[10]   G. G. Berdine, M. DiPaola, M. Weinberg, *Economic and Regulatory Perspectives on Additive Manufacturing* in *3D Printing in Orthopaedic Surgery*, Elsevier, 2019, 41-48. https://doi.org/10.1016/B978-0-323-58118-9.00004-X

[11]   S. Saedi, S. E. Saghaian, A. Jahadakbar, N. S. Moghaddam, M. T. Andani, S.M. Saghaian, Y. C. Lu, M. Elahinia, H. E. Karaca, *Materials in Medicine* **29(4)** (2018) 40. https://doi.org/10.1007/s10856-018-6044-6

[12]   A. Ahmadi, N. Shayesteh Moghaddam, M. Elahinia, H. E. Karaca, R. Mirzaeifar, *Finite Element Modeling of Selective Laser Melting 316L Stainless Steel Parts for Evaluating the Mechanical Properties* in *Proceedings of 11th International Manufacturing Science and Engineering Conference*, Blacksburg, Virginia, USA, 2016. https://doi.org/10.1115/MSEC2016-8594

[13]   S. Thakare, B. B. Ravichander, N. Swails, N. S. Moghaddam, A. Amerinatanzi, The effect of support structure geometry on surface topography of selectively laser melted parts, *Behavior and Mechanics of Multifunctional Materials IX,* SPIE Smart Structures +

Nondestructive Evaluation, Online, Proceedings Volume 11377, 2020, 113771D https://doi.org/10.1117/12.2559112

[14]   M. Zavala-Arredondo, N. Boone, J. Willmott, D. T. D. Childs, P. Ivanov, K. M. Groom, K. Mumtaz, *Materials & Design* **117** (2017) 305-315. https://doi.org/10.1016/j.matdes.2016.12.095

[15]   N. S. Moghaddam, S.Saedi, A. Amerinatanzi, E. Saghaian, A. Jahadakbar, H. Karaca, M. Elahinia, Selective laser melting of Ni-rich NiTi: selection of process parameters and the superelastic response, *SPIE Smart Structures + Nondestructive Evaluation and Health Monitoring,* Behavior and Mechanics of Multifunctional Materials and Composites XII, Proceedings Volume 10596, Denver, Colorado, USA, 2018, 105960W. https://doi.org/10.1117/12.2305247

[16]   N. S. Moghaddam, S. Saedi, A. Amerinatanzi, A. Hinojos, A. Ramazani, J. Kundin, M. J. Mills, H. Karaca, M. Elahinia, *Scientific Reports* **9** (2019) 41. https://doi.org/10.1038/s41598-018-36641-4

[17]   W. M. Tucho, P. Cuvillier, A. Sjolyst-Kverneland, V. Hansen, *Materials Science and Engineering A* **689** (2017) 220-232. https://doi.org/10.1016/j.msea.2017.02.062

[18]   J. H. Yi, J. W. Kang, T. J. Wang, X. Wang, Y. Y. Hu, T. Feng, Y. L. Feng, P. Y. Wu, *Journal of Alloys and Compounds* **786** (2019) 481-488. https://doi.org/10.1016/j.jallcom.2019.01.377

[19]   C. Prakash, S. Singh, S. Ramakrishna, *Materials Letters* **275** (2020) 128-137. https://doi.org/10.1016/j.matlet.2020.128137

[20]   G. Singh, S. Singh, C. Prakash, R. Sehgal, R. Kumar, S. Ramakrishna, *Polymer Composites* **41(9)** (2020) 3871-3891.https://doi.org/10.1002/pc.25683

[21]   N. Poomathi, S. Singh, C. Prakash, A. Subramanian, R. Sahay, A. Cinappan, S. Ramakrishna, *Rapid Prototyping Journal* **26(7)** (2020) 1313-1334. https://doi.org/10.1108/RPJ-08-2018-0217

[22]   R. Kumar, N. Ranjan, V. Kumar, R. Kumar, J. S. Chohan, A. Yadav, Piyush, S. Sharma, C. Prakash, S. Singh, C. Li, *Journal of Materials Engineering and Performance* **31** (2021) 2391-2409. https://doi.org/10.1007/s11665-021-06329-4

[23]   B. Ahmad, S. O. van der Veen, M. E. Fitzpatrick, H. Guo, *Additive Manufacturing* **22** (2018) 571-582. https://doi.org/10.1016/j.addma.2018.06.002